Astrophysical models to interpret the Pierre Auger Observatory data

Juan Manuel González for the Pierre Auger Collaboration

CONICET

PIERRE AUGER OBSERVATORY

MOTIVATION

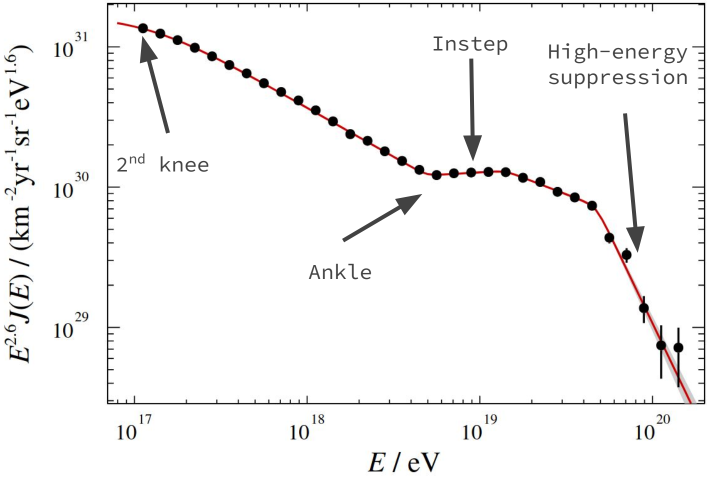

Eur. Phys JC 81 (2021) 966

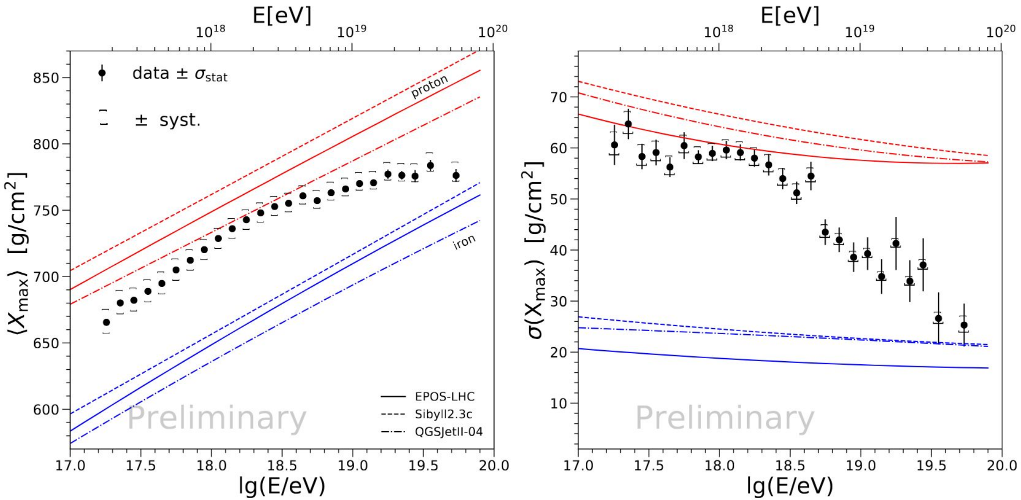

A. Yushkov, for Auger, PoS ICRC2019 (2020) 482

- Pierre Auger Observatory measurements of the spectrum and composition show several features
- Which is their origin?
- We want to infer the source properties for some simple astrophysical scenarios

COMBINED FIT OF SPECTRUM AND COMPOSITION

1) Model of the sources

$$\dot{Q}(z,E) = \dot{Q}_0 \xi(z) \sum_A f_A \left(\frac{E}{E_0}\right)^{-\gamma} f_{\text{cut}} \left(\frac{E}{Z_A R_{\text{cut}}}\right)$$

Source evolution $\xi(z) = (1+z)^m$

5 elements (H, He, N, Si, Fe)

$$f(E, Z_A, R_{\text{cut}}) = \begin{cases} 1 & E \leqslant Z_A R_{\text{cut}} \\ \exp\left(1 - \frac{E}{Z_A R_{\text{cut}}}\right) & E > Z_A R_{\text{cut}} \end{cases}$$

2) CRs propagated with SimProp (*JCAP 11 (2017) 009*): interactions with CMB & Gilmore EBL radiation backgrounds, TALYS photodisintegration

3) Air shower interactions modelled with EPOS-LHC or Sibyll2.3d

DATASETS ($E > 10^{17.8}$ eV)

SPECTRUM (N_{data}= 24)

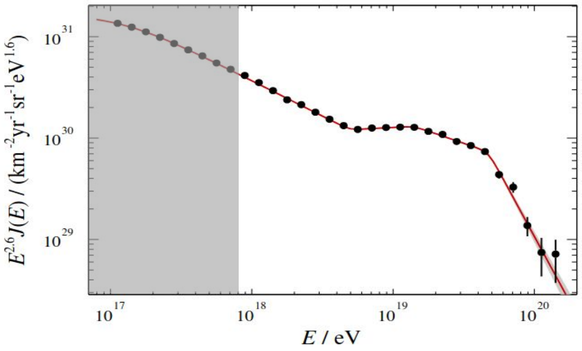

Eur. Phys JC 81 (2021) 966

X_{max} DISTRIBUTIONS (N_{data}= 329)

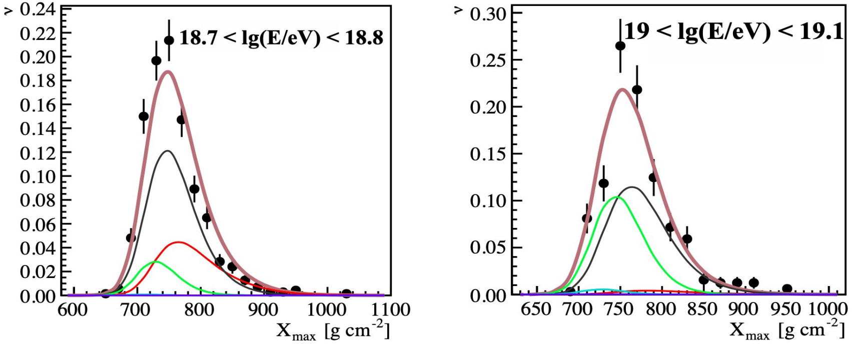

A. Yushkov, for Auger, PoS ICRC2019 (2020) 482

Fit Procedure

$$L_J = \prod_i \frac{1}{\sqrt{2\pi\sigma_i^2}} \exp\left(-\frac{(J_i^{mod} - J_i^{obs})^2}{2\sigma_i^2}\right)$$

$$L_{X_{\max}} = \prod_i n_i^{obs} \prod_j \frac{1}{k_{i,j}^{obs}} (G_{i,j}^{mod})^{k_{i,j}^{obs}}$$

$G_{i,j}^{mod}$: *Gumbel + resolution & acceptance*

Minimize the deviance

$$D = -2ln\left(\frac{L_J}{L_J^{sat}}\right) - 2ln\left(\frac{L_{X_{max}}}{L_{X_{max}}^{sat}}\right)$$

- Fit parameters: γ, R_{cut} and elemental fractions for both components

REFERENCE SCENARIOS

JCAP 05(2023)024

Scenario 1 (γ_G=2.7)

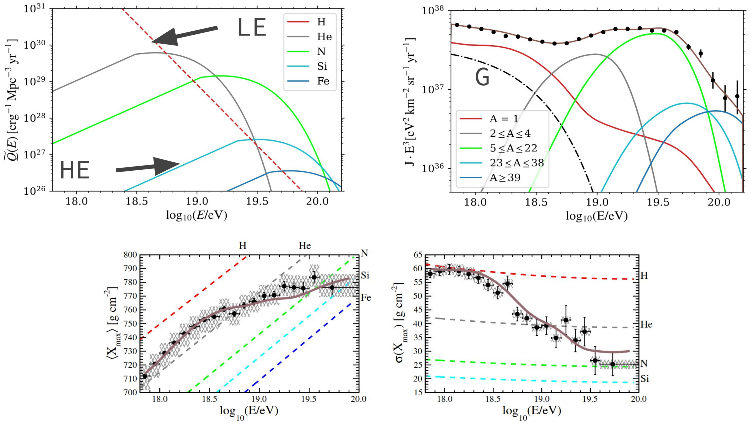

Scenario 2

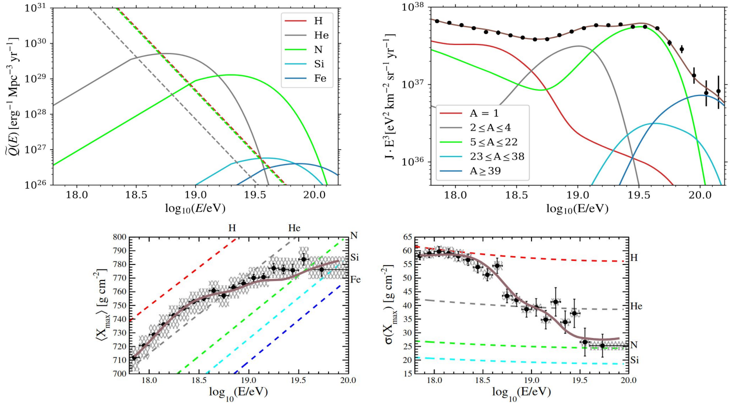

	Scenario 1		Scenario 2	
Galactic contribution (at Earth)	pure N		—	
$J_0^{Gal}/(\mathrm{eV}^{-1}\,\mathrm{km}^{-2}\,\mathrm{sr}^{-1}\,\mathrm{yr}^{-1})$	$(1.06 \pm 0.04)\times 10^{-13}$		—	
$\log_{10}(R_{cut}^{Gal}/\mathrm{eV})$	17.48 ± 0.02		—	
EG components (at the escape)	LE	HE	LE	HE
$L_0/(10^{44}\,\mathrm{erg\,Mpc^{-3}\,yr^{-1}})$	6.54 ± 0.36	5.00 ± 0.35	11.35 ± 0.15	5.07 ± 0.06
γ	3.34 ± 0.07	-1.47 ± 0.13	3.52 ± 0.03	-1.99 ± 0.11
$\log_{10}(R_{cut}/\mathrm{eV})$	>19.3	18.19 ± 0.02	>19.4	18.15 ± 0.01
$I_H(\%)$	100 (fixed)	0.0 ± 0.0	48.7 ± 0.3	0.0 ± 0.0
$I_{He}(\%)$	—	24.5 ± 3.0	7.3 ± 0.4	23.6 ± 1.6
$I_N(\%)$	—	68.1 ± 5.0	44.0 ± 0.4	72.1 ± 3.3
$I_{Si}(\%)$	—	4.9 ± 3.9	0.0 ± 0.0	1.3 ± 1.3
$I_{Fe}(\%)$	—	2.5 ± 0.2	0.0 ± 0.0	3.1 ± 1.3
$D_J\ (N_J)$	48.6 (24)		56.6 (24)	
$D_{X_{max}}\ (N_{X_{max}})$	537.4 (329)		516.5 (329)	
$D\ (N)$	586.0 (353)		573.1 (353)	

- **Hard HE spectra (γ<-1.5)**
- **Instep** due to **He suppression**
- **N** flux **dominates** the **above the instep**
- **Si** and **Fe dominate** at the **highest energies**
- Pure proton LE composition with a N-dominated Galactic component better describes spectrum data
- **Mixed LE composition** with **no galactic** component **better describes** all **data**

SOURCES' COSMOLOGICAL EVOLUTION

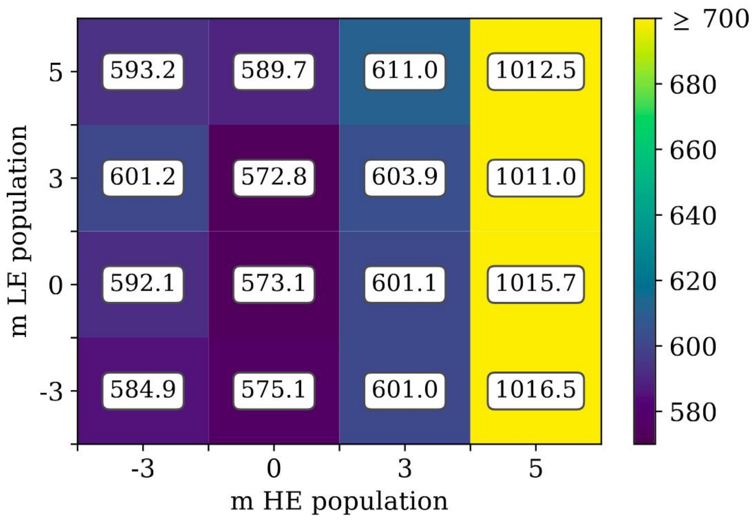

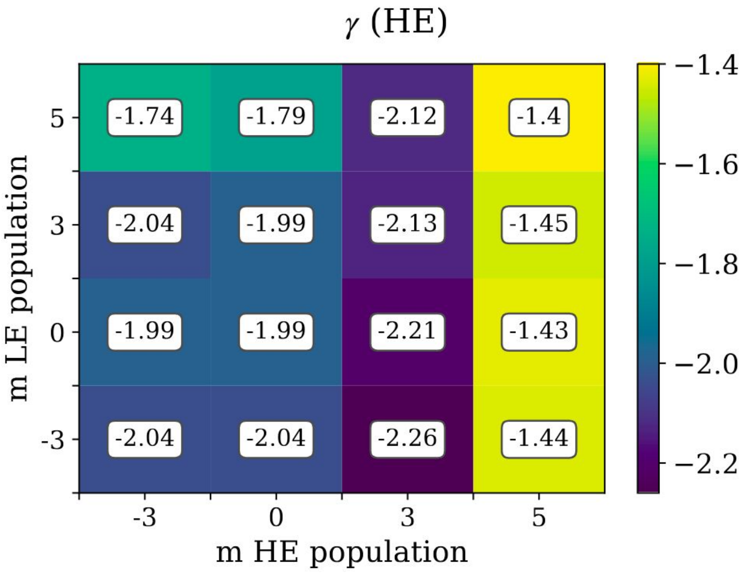

- **Strong HE evolution disfavoured** (too many secondaries)
- **m=0 HE** & **m=3 LE** evolution slightly **favoured**
- **Hard HE spectrum** for all the cosmological evolutions considered **(γ<−1.4)**

INCLUDING THE MAGNETIC HORIZON EFFECT

SPECTRUM AT THE SOURCES

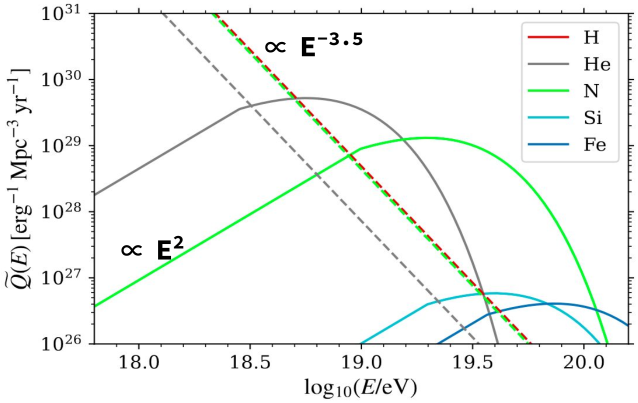

PROPAGATION

SPECTRUM AT EARTH

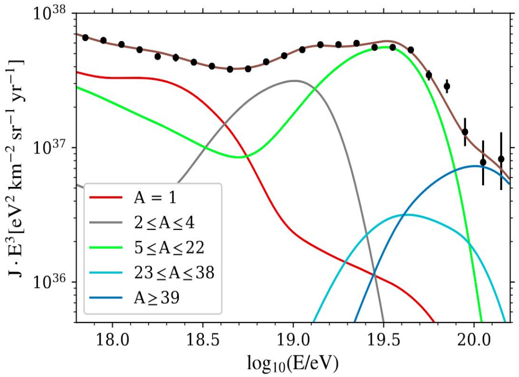

DEPTH OF SHOWER MAXIMA

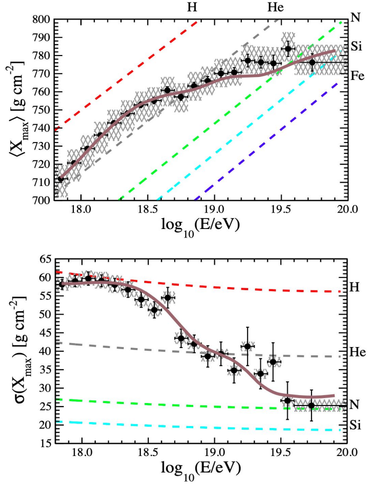

- Very **hard spectrum required** for the **high-energy component**
- Can we explain this as a consequence of the **magnetic horizon effect** (MHE)?
- We know sources must have a finite density & that Extra-Galactic Magnetic Fields are present
- MHE: Low energy particles do not reach Earth if the diffusion time from the closest sources is larger than the age of the sources

MAGNETIC HORIZON EFFECT

- Extragalactic magnetic fields (EGMF) between Earth and closest sources modelled as ***turbulent & isotropic*** with rms amplitude (***B_{rms}***) & coherence length (***L_{coh}***)
- Critical energy E_{crit} such that: $r_L(E_{crit}) = L_{coh} \longrightarrow R_{crit} \equiv E_{crit}/Z = 0.9 \frac{B_{rms}}{nG} \frac{L_{coh}}{Mpc} \mathrm{EeV}$
- Uniform source density, intersource distance d_s
- MHE suppresses the flux at low energies

$$J_Z(E) = G(E/E_{crit}) J_Z|_{d_s \to 0}$$

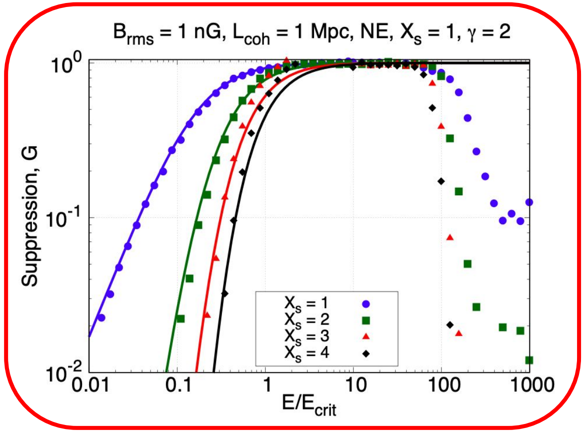

$$G(x) = \exp\left[-\left(\frac{aX_s}{x + b(x/a)^\beta}\right)^\alpha\right]$$

X_s: normalized distance

$$X_s = \frac{d_s}{\sqrt{r_H L_{coh}}} \simeq \frac{d_s}{25\,\mathrm{Mpc}} \sqrt{\frac{\mathrm{Mpc}}{L_{coh}}}$$

$r_H = c/H_0$

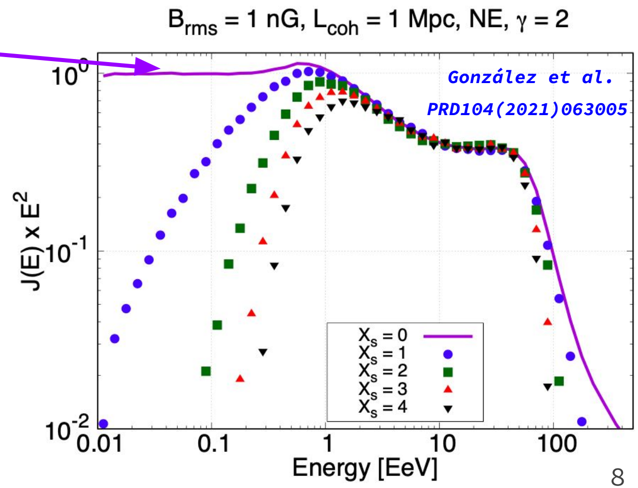

Proton flux at Earth.

COMBINED FIT OF SPECTRUM AND COMPOSITION

1) Model of the sources

$$\dot{Q}(z,E) = \dot{Q}_0 \xi(z) \sum_A f_A \left(\frac{E}{E_0}\right)^{-\gamma} f_{\text{cut}}\left(\frac{E}{Z_A R_{\text{cut}}}\right)$$

Δ: steepness of the cutoff (1, 2, or 3)

5 elements (H, He, N, Si, Fe)

2) CRs propagated with SimProp (*JCAP 11 (2017) 009*): interactions with CMB & Gilmore EBL radiation backgrounds, TALYS photodisintegration

4) Air shower interactions modelled with EPOS-LHC or Sibyll2.3d

COMBINED FIT OF SPECTRUM AND COMPOSITION

1) Model of the sources

$$\dot{Q}(z,E) = \dot{Q}_0 \xi(z) \sum_A f_A \left(\frac{E}{E_0}\right)^{-\gamma} f_{\rm cut}\left(\frac{E}{Z_A R_{\rm cut}}\right)$$

Source evolution ξ(z): no evolution (NE) or star formation rate (SFR)

$$f_{\rm cut}(E, Z_A, R_{\rm cut}) = \mathrm{sech}\left[\left(\frac{\mathrm{E}}{\mathrm{Z_A R_{cut}}}\right)^{\Delta}\right]$$

Δ: steepness of the cutoff (1, 2, or 3)

5 elements (H, He, N, Si, Fe)

2) CRs propagated with SimProp (*JCAP 11 (2017) 009*): interactions with CMB & Gilmore EBL radiation backgrounds, TALYS photodisintegration

3) Account for EGMF multiplying by the suppression factor $G(E/E_{crit}, X_s)$

4) Air shower interactions modelled with EPOS-LHC or Sibyll2.3d

FIT INCLUDING MHE AS A FUNCTION OF X_S

JCAP07(2024)094

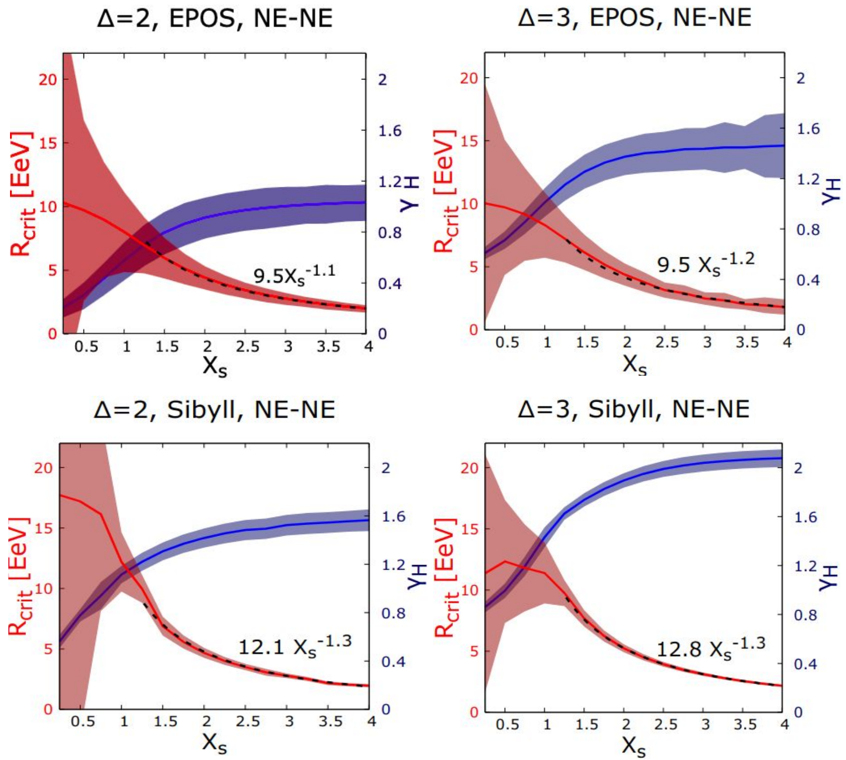

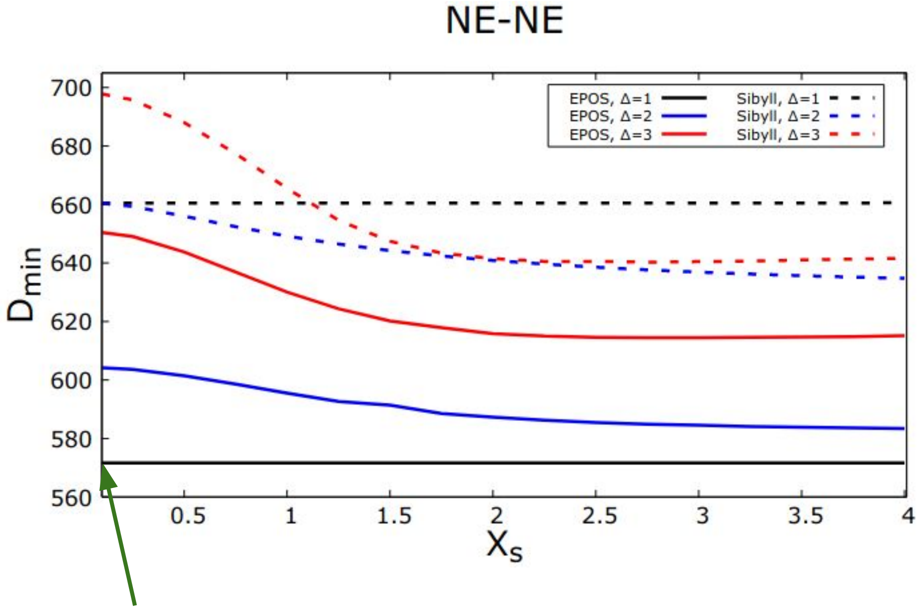

≡ no B

- **Larger X_s** results in **softer spectra** and **smaller R_{crit}**
- When MHE is relevant (X_s > 1), best fit for **$X_s R_{crit}$~ 10 EeV**
- Deviance is almost degenerate for $X_s \geq 2$

BEST FIT RESULTS

with EGMF, NE-NE

Δ	EPOS-LHC							Sibyll 2.3d						
	γ_H	R^H_{cut} [EeV]	γ_L	R^L_{cut} [EeV]	X_s	R_{crit} [EeV]	D ($N=353$)	γ_H	R^H_{cut} [EeV]	γ_L	R^L_{cut} [EeV]	X_s	R_{crit} [EeV]	D ($N=353$)
1	−2.19	1.35	3.54	> 60	0	–	572	−1.67	1.42	3.37	2.21	0	–	660
2	1.03	6.02	3.62	> 51	> 3.2	1.97	583	1.35	6.22	3.53	> 25	> 3.1	1.54	635
3	1.43	7.50	3.69	> 61	2.8	2.79	614	2	7.50	3.62	> 31	2.6	3.77	640
							SFR-NE							
1	−2.09	1.39	3.24	> 63	0	–	578	−1.64	1.44	3.03	2.89	0	–	665
2	1.12	6.14	3.33	> 61	> 3.5	2.11	586	1.45	6.29	3.21	> 37	> 3.2	1.67	635
3	1.49	7.52	3.41	> 57	2.7	3.15	617	2.07	7.49	3.31	> 33	2.8	3.52	637

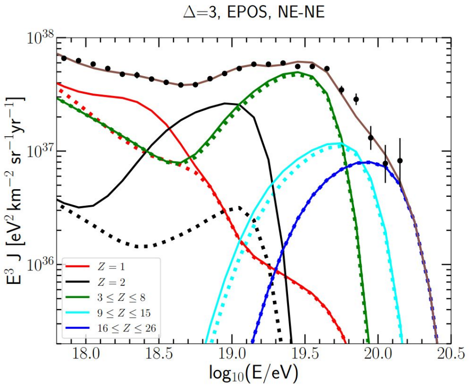

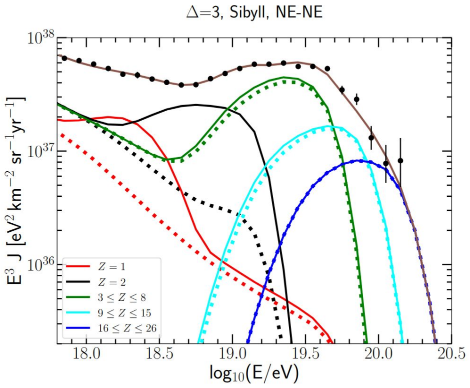

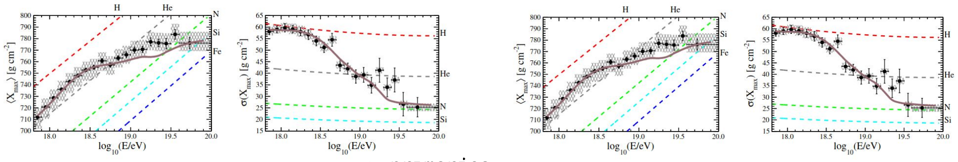

▪ ▪ ▪ primaries

▬ primaries + secondaries

- **Δ=1 cutoff** leads to **results close** to the case with **B=0**
- **Steeper cutoffs**, produce **softer HE spectra (γ>1)**
- **Sibyll, Δ=3** produces a **HE spectrum reaching γ=2,** consistent with expectations from diffusive shock acceleration
- **SFR evolution** of the **LE component** hardens the spectrum by about 0.3 units with a **small effect in deviance**

EFFECT OF SYSTEMATIC UNCERTAINTIES

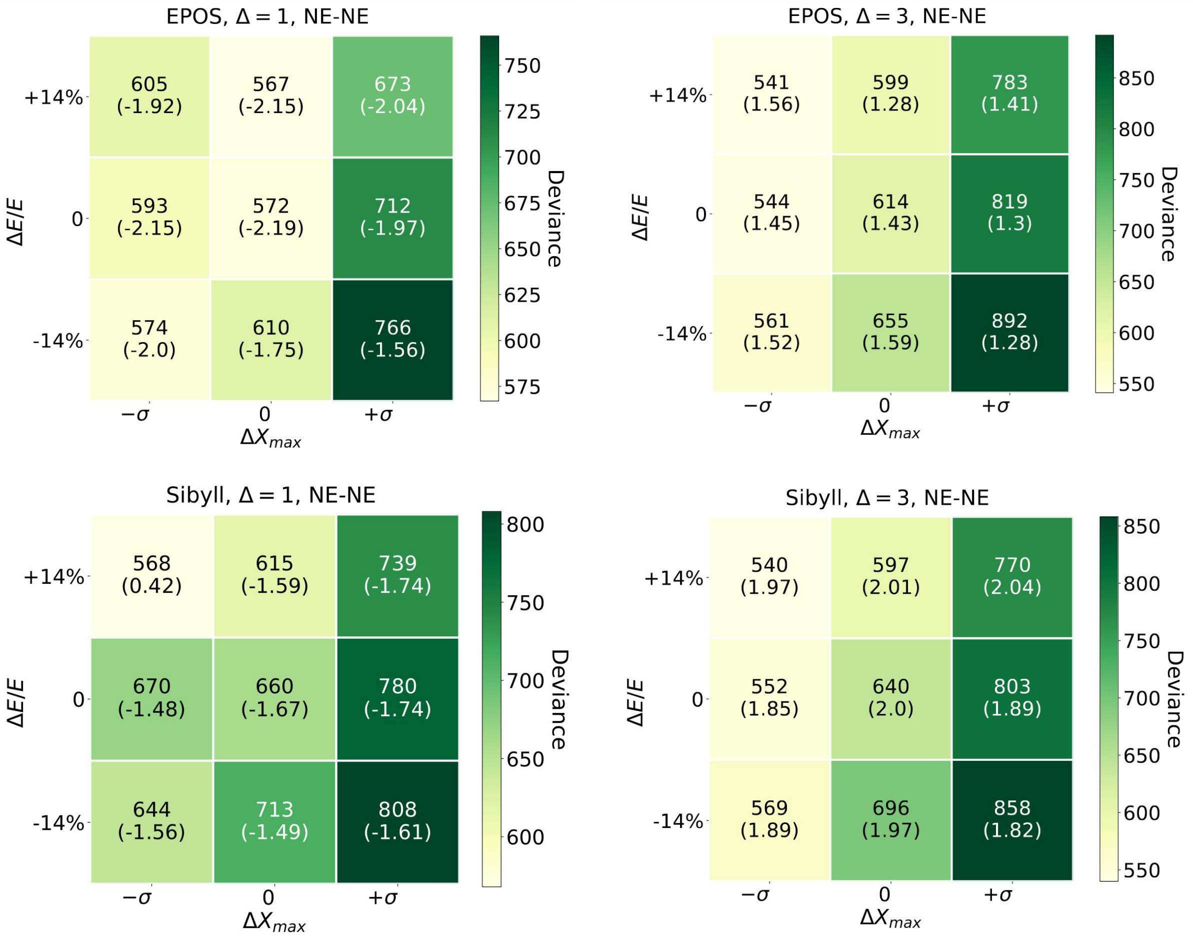

- When including EGMF the **fit generally improves** for a **positive shift in energy and a negative shift in X_{max}**
- The **smallest deviance** is reached for **Δ=3 cutoff, ΔE/E=+14% & ΔX_{max}=−σ**
- $\gamma_H \approx 2$ for **best fit** scenarios
- **Positive shifts** in X_{max} are **disfavoured** by about a 100 units

EFFECT OF SYSTEMATIC UNCERTAINTIES

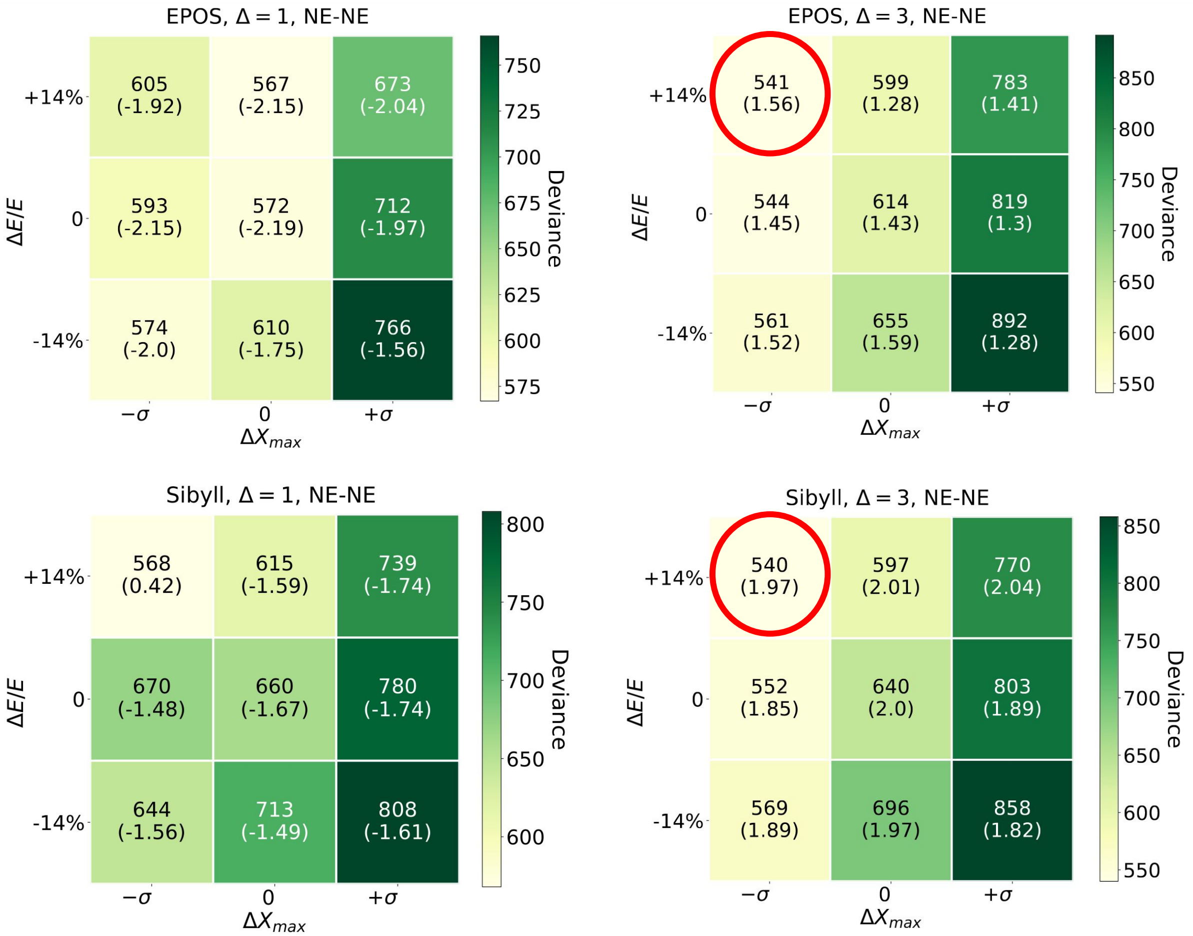

- When including EGMF the **fit generally improves** for a **positive shift in energy and a negative shift in X_{max}**
- The **smallest deviance** is reached for **Δ=3 cutoff, ΔE/E=+14% & ΔX_{max}=−σ**
- $\gamma_H \approx 2$ for **best fit** scenario
- **Positive shifts** in X_{max} are **disfavoured** by about a 100 units

SMALL SCALE ANISOTROPIES IN ARRIVAL DIRECTIONS (AD)

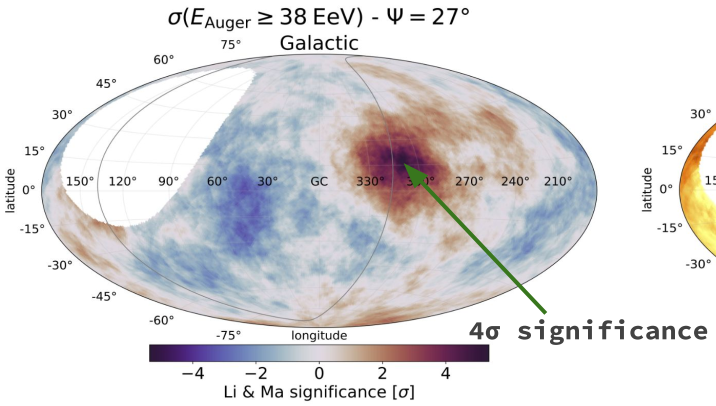

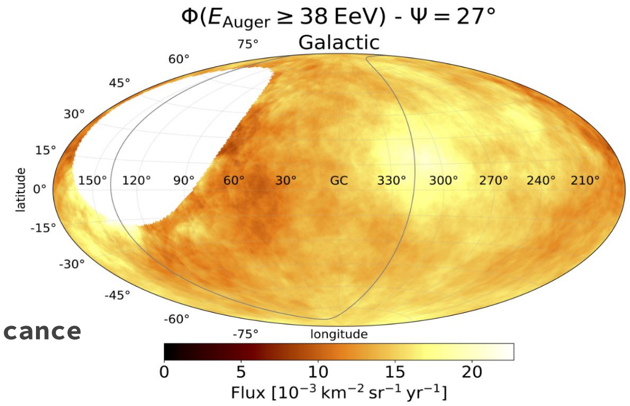

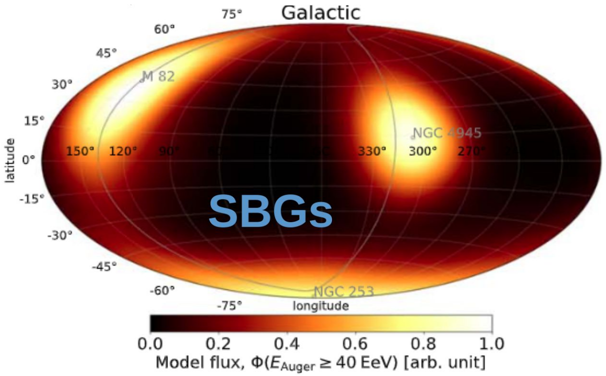

SBG (*JCAP 2019 (2019) 073*)

- Most significant anisotropy above 32 EeV in the CenA region, where also some starburst galaxies (SBG) lie
- Look for best fit to spectrum + composition + AD flux maps from possible source catalogs

INCLUDING THE ARRIVAL DIRECTIONS IN THE COMBINED FIT

JCAP01(2024)022

Energy spectrum

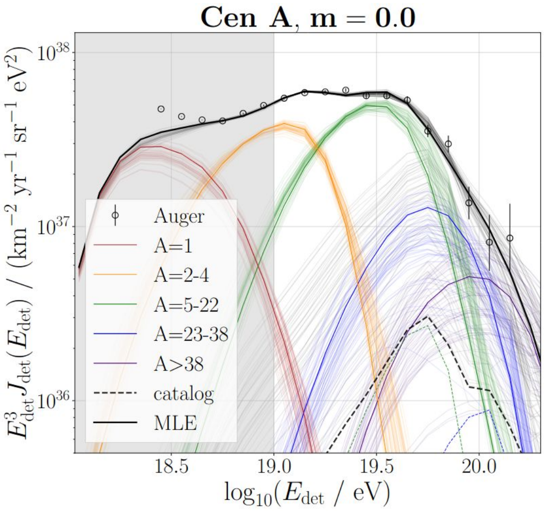

X_{max} distributions

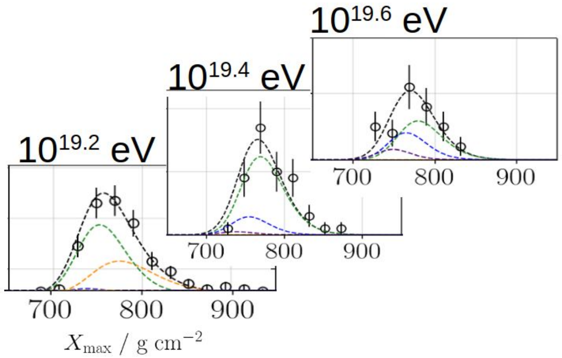

arrival directions

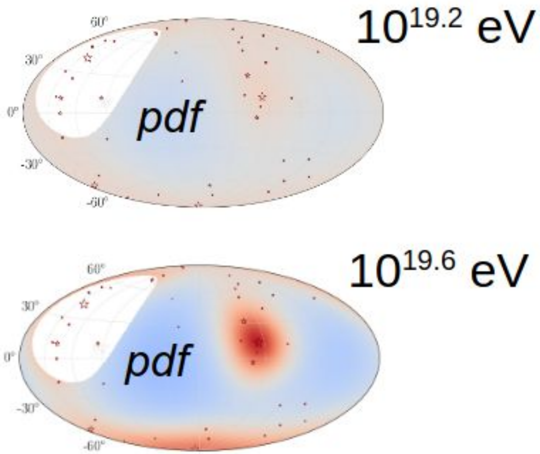

- Poissonian likelihood
- Spectrum fitted above 10 EeV

- Modified Gumbel functions to include resolution & acceptance
- Multinomial likelihood
- EPOS-LHC model
- E > 10 EeV

- Construct flux maps for each energy bin
- Contrast with arrival direction data
- E > 16 EeV

SIGNAL FRACTION & ARRIVAL DIRECTIONS

- Model parameters:
  - signal fraction at 40 EeV $\mathbf{f_0}$
    - catalogue contribution (energy dependent)
  - arrival direction blurring due to magnetic fields (rigidity dependent)

$$\delta = \frac{\delta_0}{R/10EeV}$$

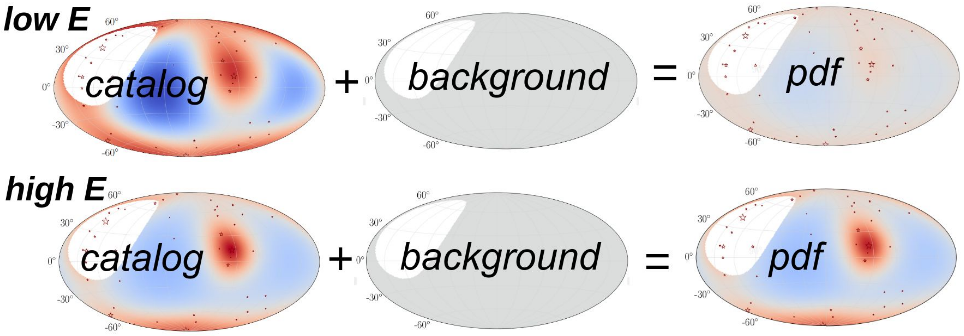

RESULTS

	Cen A, $m=0$ (flat)		Cen A, $m=3.4$ (SFR)		SBG, $m=3.4$ (SFR)	
	posterior	MLE	posterior	MLE	posterior	MLE
γ	$-1.67^{+0.48}_{-0.47}$	-2.21	$-3.09^{+0.23}_{-0.24}$	-3.05	$-2.77^{+0.27}_{-0.29}$	-2.67
$\log_{10}(R_{\rm cut}/{\rm V})$	$18.23^{+0.04}_{-0.06}$	18.19	$18.10^{+0.02}_{-0.02}$	18.11	$18.13^{+0.02}_{-0.02}$	18.13
f_0	$0.16^{+0.06}_{-0.14}$	0.028	$0.05^{+0.01}_{-0.03}$	0.028	$0.17^{+0.06}_{-0.08}$	0.19
$\delta_0/°$	$56.5^{+29.4}_{-12.8}$	16.5	$27.6^{+2.7}_{-16.3}$	16.8	$22.2^{+5.3}_{-4.0}$	24.3
$I_{\rm H}$	$5.9^{+2.5}_{-1.7}\times10^{-2}$	7.1×10^{-2}	$8.3^{+2.0}_{-8.3}\times10^{-3}$	1.6×10^{-5}	$6.4^{+1.3}_{-6.4}\times10^{-3}$	4.3×10^{-5}
$I_{\rm He}$	$2.3^{+0.3}_{-0.5}\times10^{-1}$	1.9×10^{-1}	$1.3^{+0.2}_{-0.2}\times10^{-1}$	1.4×10^{-1}	$1.7^{+0.3}_{-0.4}\times10^{-1}$	1.8×10^{-1}
$I_{\rm N}$	$6.3^{+0.3}_{-0.3}\times10^{-1}$	6.2×10^{-1}	$7.4^{+0.3}_{-0.3}\times10^{-1}$	7.3×10^{-1}	$7.4^{+0.3}_{-0.3}\times10^{-1}$	7.4×10^{-1}
$I_{\rm Si}$	$6.5^{+3.6}_{-3.3}\times10^{-2}$	9.9×10^{-2}	$9.2^{+3.2}_{-2.3}\times10^{-2}$	1.1×10^{-1}	$5.7^{+2.5}_{-3.1}\times10^{-2}$	5.4×10^{-2}
$I_{\rm Fe}$	$1.6^{+0.7}_{-1.0}\times10^{-2}$	2.0×10^{-2}	$2.5^{+0.8}_{-0.9}\times10^{-2}$	2.3×10^{-2}	$2.5^{+0.8}_{-0.9}\times10^{-2}$	2.3×10^{-2}
$\log b$	-264.0 ± 0.2		-272.6 ± 0.2		-266.9 ± 0.1	
D_E ($N_J=14$)		22.3		28.5		33.3
$D_{X_{\rm max}}$ ($N_{X_{\rm max}}=74$)		124.9		130.6		126.2
D		147.2		159.1		159.5
$\log \mathcal{L}_{\rm ADs}$		10.5		10.4		13.3
$\log \mathcal{L}$		-239.1		-245.1		-242.4

- CenA with flat evolution offers the best description of the data
- Hard spectral index
- catalogue contribution at 40 EeV between ~3% and 20%
- $\delta_0 > 10^0$ magnetic blurring for all scenarios
- Composition dominated by mid-mass nuclei

RESULTS

	Cen A, $m = 0$ (flat)		Cen A, $m = 3.4$ (SFR)		SBG, $m = 3.4$ (SFR)	
	posterior	MLE	posterior	MLE	posterior	MLE
γ	$-1.67^{+0.48}_{-0.47}$	-2.21	$-3.09^{+0.23}_{-0.24}$	-3.05	$-2.77^{+0.27}_{-0.29}$	-2.67
$\log_{10}(R_{cut}/V)$	$18.23^{+0.04}_{-0.06}$	18.19	$18.10^{+0.02}_{-0.02}$	18.11	$18.13^{+0.02}_{-0.02}$	18.13
f_0	$0.16^{+0.06}_{-0.14}$	0.028	$0.05^{+0.01}_{-0.03}$	0.028	$0.17^{+0.06}_{-0.08}$	0.19
$\delta_0/°$	$56.5^{+29.4}_{-12.8}$	16.5	$27.6^{+2.7}_{-16.3}$	16.8	$22.2^{+5.3}_{-4.0}$	24.3
I_H	$5.9^{+2.5}_{-1.7} \times 10^{-2}$	7.1×10^{-2}	$8.3^{+2.0}_{-8.3} \times 10^{-3}$	1.6×10^{-5}	$6.4^{+1.3}_{-6.4} \times 10^{-3}$	4.3×10^{-5}
I_{He}	$2.3^{+0.3}_{-0.5} \times 10^{-1}$	1.9×10^{-1}	$1.3^{+0.2}_{-0.2} \times 10^{-1}$	1.4×10^{-1}	$1.7^{+0.3}_{-0.4} \times 10^{-1}$	1.8×10^{-1}
I_N	$6.3^{+0.3}_{-0.3} \times 10^{-1}$	6.2×10^{-1}	$7.4^{+0.3}_{-0.3} \times 10^{-1}$	7.3×10^{-1}	$7.4^{+0.3}_{-0.3} \times 10^{-1}$	7.4×10^{-1}
I_{Si}	$6.5^{+3.6}_{-3.3} \times 10^{-2}$	9.9×10^{-2}	$9.2^{+3.2}_{-2.3} \times 10^{-2}$	1.1×10^{-1}	$5.7^{+2.5}_{-3.1} \times 10^{-2}$	5.4×10^{-2}
I_{Fe}	$1.6^{+0.7}_{-1.0} \times 10^{-2}$	2.0×10^{-2}	$2.5^{+0.8}_{-0.9} \times 10^{-2}$	2.3×10^{-2}	$2.5^{+0.8}_{-0.9} \times 10^{-2}$	2.3×10^{-2}
$\log b$	-264.0 ± 0.2		-272.6 ± 0.2		-266.9 ± 0.1	
D_E ($N_J = 14$)		22.3		28.5		33.3
$D_{X_{max}}$ ($N_{X_{max}} = 74$)		124.9		130.6		126.2
D		147.2		159.1		159.5
$\log \mathcal{L}_{ADs}$		10.5		10.4		13.3
$\log \mathcal{L}$		-239.1		-245.1		-242.4

- CenA with flat evolution offers the best description of the data
- Hard spectral index
- catalogue contribution at 40 EeV between ~3% and 20%
- $\delta_0 > 10^0$ magnetic blurring for all scenarios
- Composition dominated by mid-mass nuclei

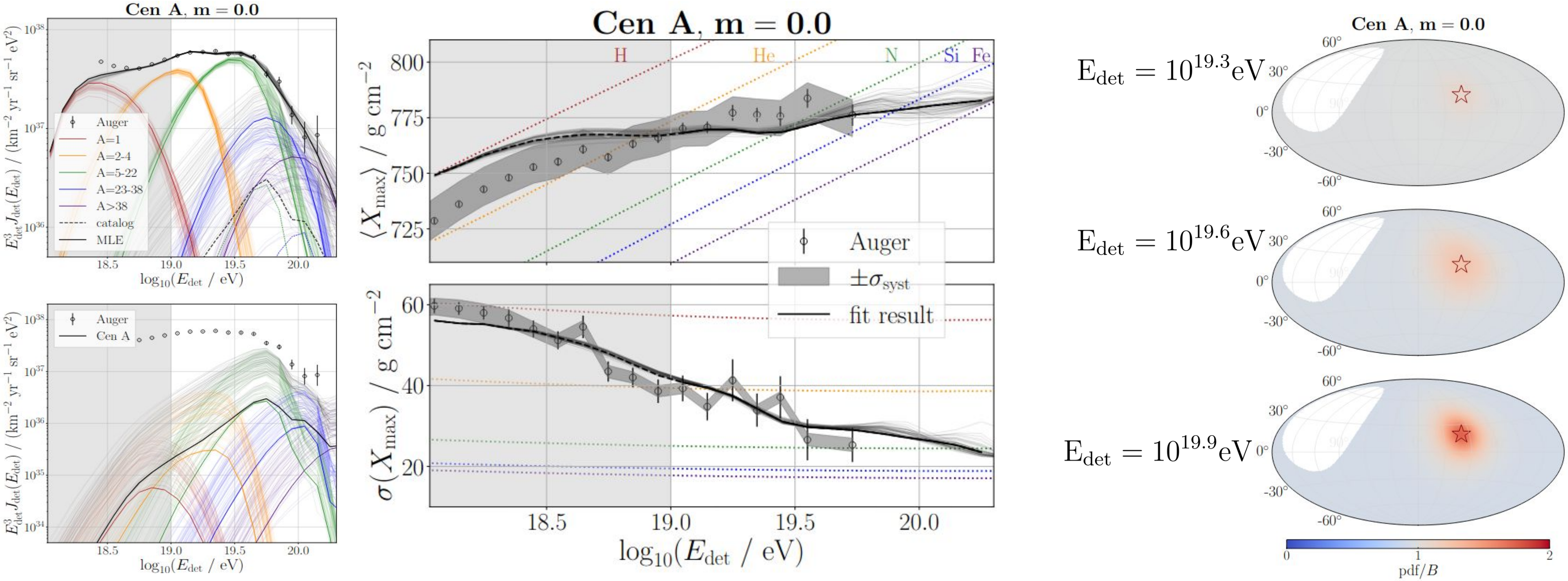

- Cen A contribution to the flux grows with energy (reaches ~10%) with large uncertainties

CONCLUSIONS

- The observed features of the **spectrum and composition data** can be described with **two mixed composition extragalactic components**

- Hard HE spectrum & flat cosmological source evolutions are favoured if MHE is not included

- For **Δ=2 & 3 and X_s ≳ 2** we found scenarios where the magnetic horizon plays an important role with **better deviance than for B=0**, and with **softer spectral index for the HE component (γ ∈ [1,2])**

- **Sibyll2.3d** leads to **spectral indices** for the **HE component close to 2 when MHE is included**

- Requires **large inter-source distances and strong magnetic fields** between us and the closest sources

$$X_s R_{crit} \simeq 5 \text{ EeV} \frac{d_s}{20 \text{ Mpc}} \frac{B_{rms}}{50 \text{ nG}} \sqrt{\frac{L_{coh}}{100 \text{ kpc}}}$$

- **Catalogue sources** contribute between **~3% to ~20%** to the **flux at 40 EeV**

- Magnetic blurring for protons at 10 EeV $\delta_0 > 10^0$

Thank you!

Backup slides

NEUTRINOS' FLUX

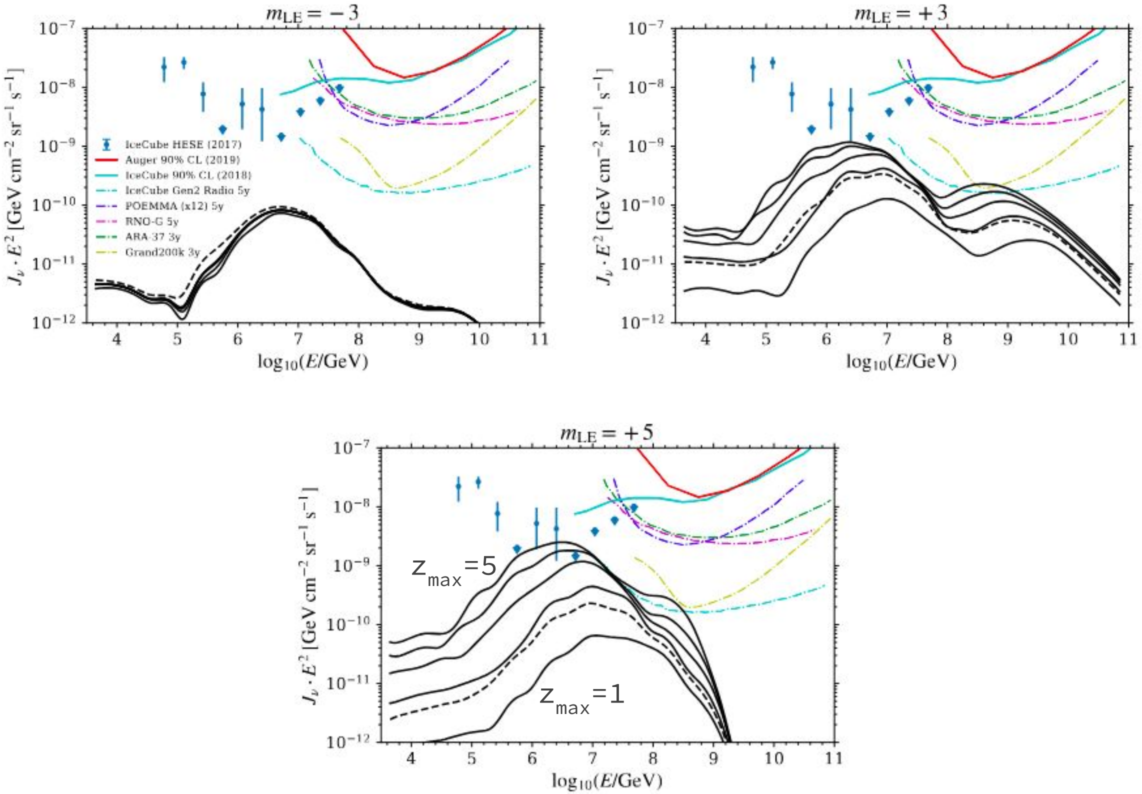

- m_{HE}=0 for all scenarios
- Dominant contribution from LE component, which has steep spectrum and large cutoff
- Peak at 10^7 GeV due to pion-photoproduction on the EBL
- For realistic scenarios, predicted flux lower than present observations

Effect of the cutoff shape on the injected spectra

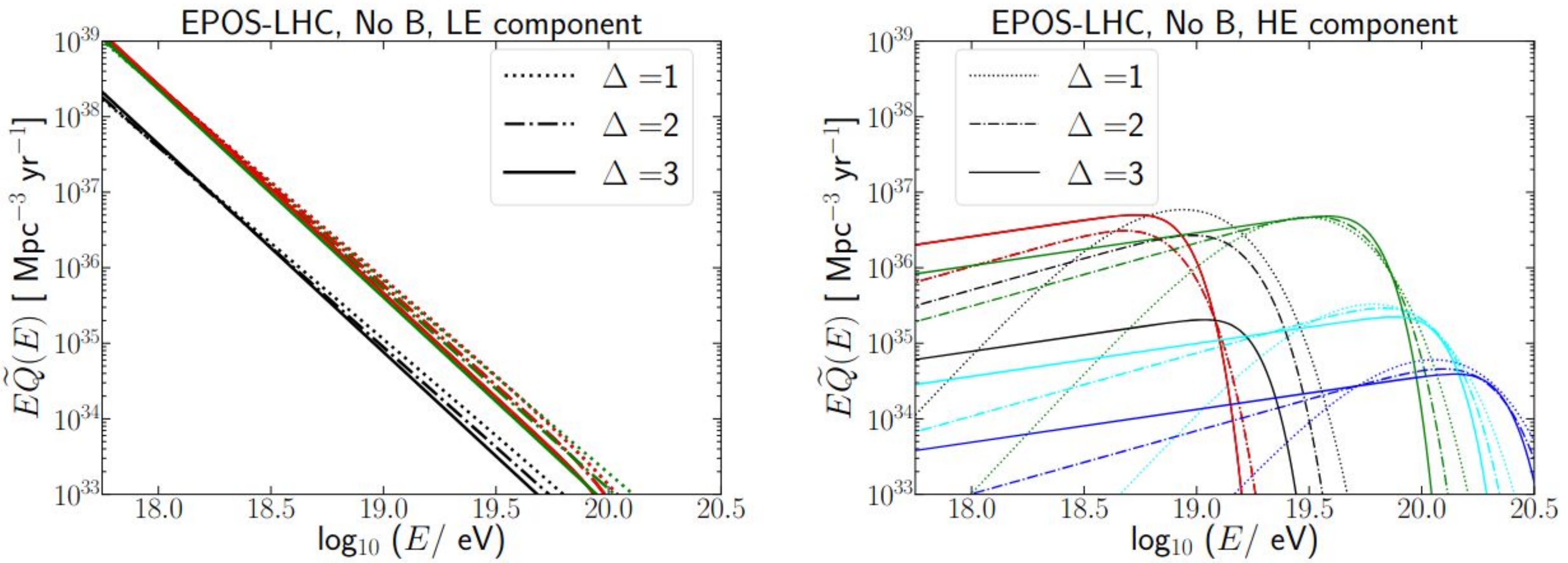

Notice how the parameters combine to produce a similar shape at the energy at which each element is dominant

EXTRAGALACTIC MAGNETIC FIELDS EXPECTATIONS

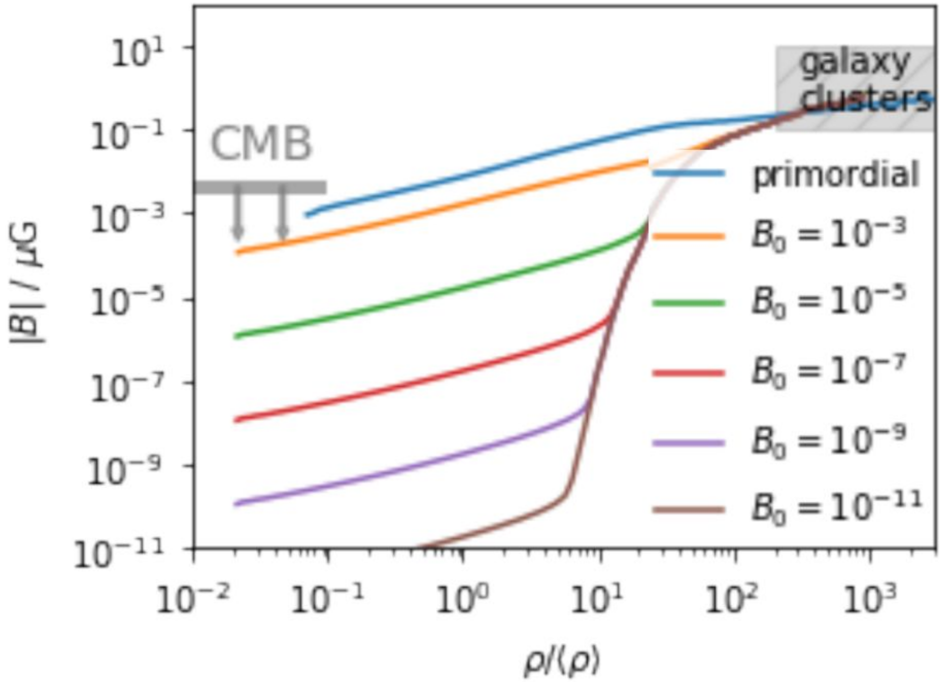

Median magnetic field strength $|B|$ as function of over-density $\rho/\langle\rho\rangle$ for a number of MHD models with identical dynamo physics, starting with different strengths of the primordial magnetic field B0 , indicated by the label in μG

Hackstein, Brüggen, Vazza & Rodrigues, MNRAS (2020) 498 4811

Required magnetic fields close to the maximum values

B_{rms} vs. L_{coh}

$$X_s R_{crit} \simeq 5\ \mathrm{EeV} \frac{d_s}{20\,\mathrm{Mpc}} \frac{B_{rms}}{50\,\mathrm{nG}} \sqrt{\frac{L_{coh}}{100\,\mathrm{kpc}}}$$

$$d_s > 20\mathrm{Mpc}\sqrt{\frac{\mathrm{L_{coh}}}{100\mathrm{kpc}}}$$

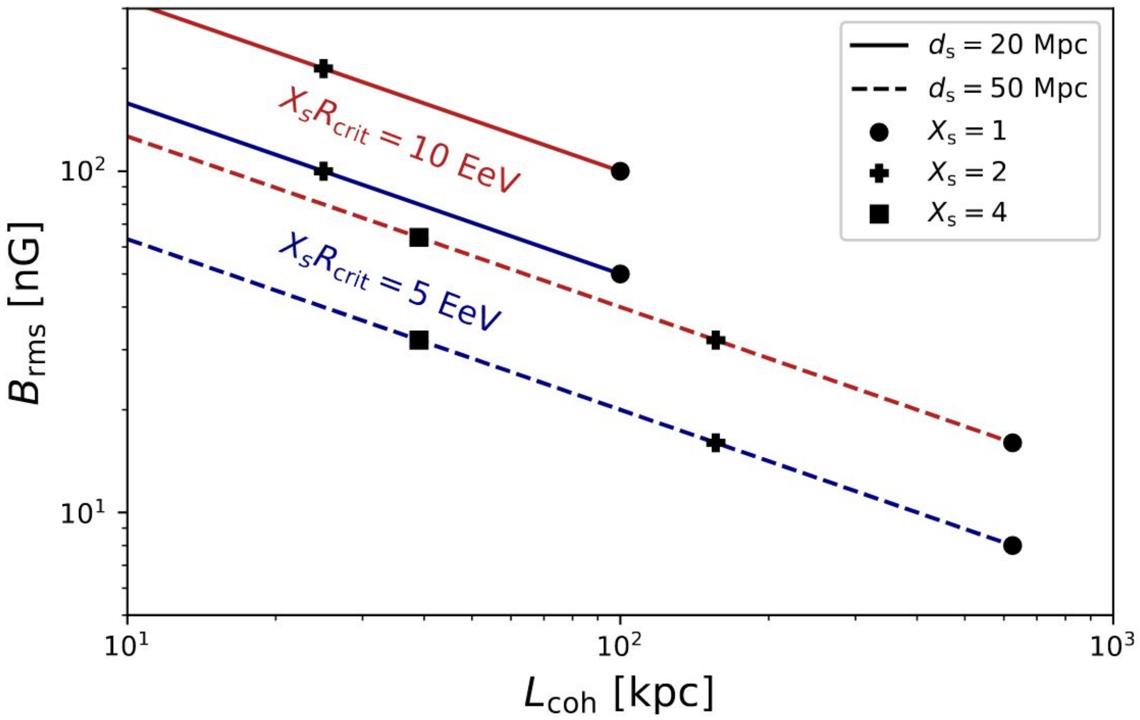

- Scenarios with magnetic horizon require strong magnetic fields within the Local Supercluster and large inter-source separation (low source density)

γ-AGN MODEL

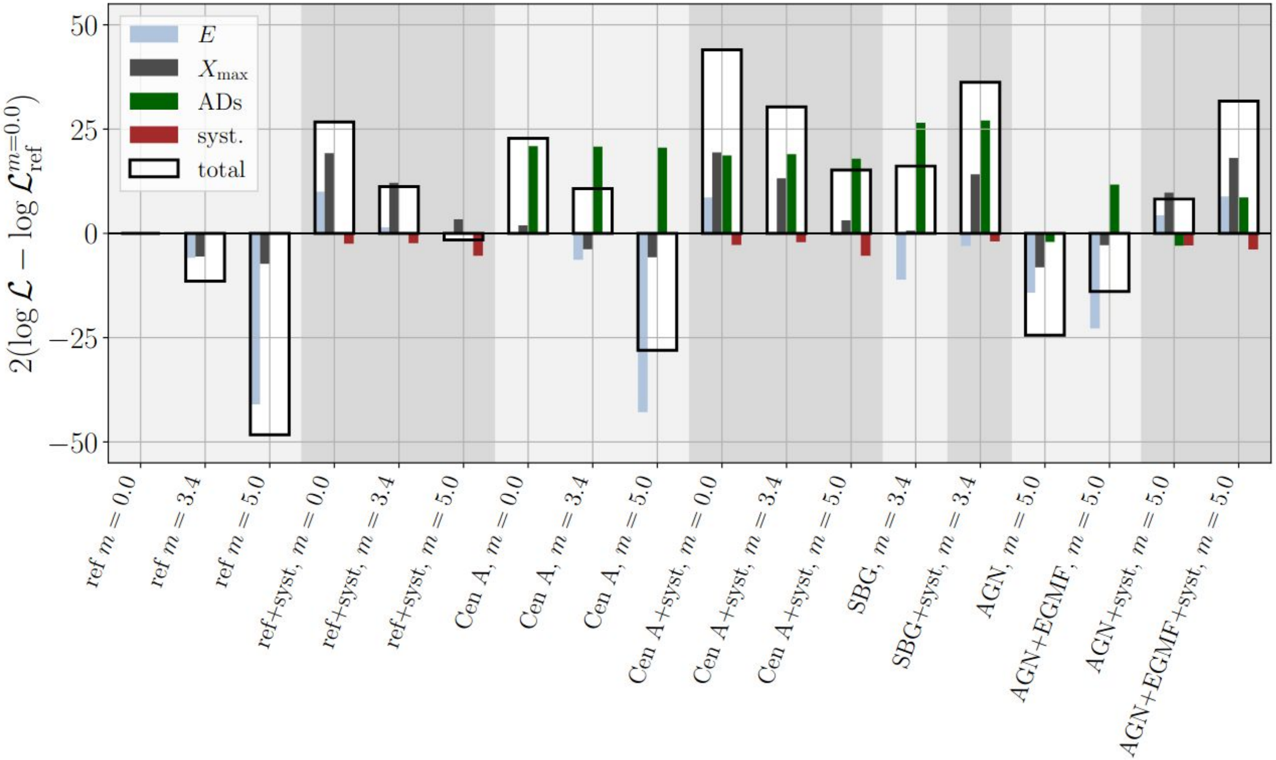

- AGN model worsens the fit (smaller likelihood)
- $\gamma \approx -3.5$ (very hard)
- $f_0 \approx 15\%$, γ-AGN catalogue dominated by blazar Markarian 421
- Can’t explain arrival directions better, even including an EGMF

Astropart. Phys. 5 (1996) 279